

PAPER • OPEN ACCESS

## Energetic cost of quantum control protocols

To cite this article: Obinna Abah *et al* 2019 *New J. Phys.* **21** 103048

View the [article online](#) for updates and enhancements.



## PAPER




## Energetic cost of quantum control protocols

## OPEN ACCESS

RECEIVED  
21 June 2019REVISED  
19 September 2019ACCEPTED FOR PUBLICATION  
9 October 2019PUBLISHED  
28 October 2019

Original content from this work may be used under the terms of the [Creative Commons Attribution 3.0 licence](https://creativecommons.org/licenses/by/4.0/).

Any further distribution of this work must maintain attribution to the author(s) and the title of the work, journal citation and DOI.

Obinna Abah<sup>1</sup>, Ricardo Puebla<sup>1</sup>, Anthony Kiely<sup>2,3</sup>, Gabriele De Chiara<sup>1</sup> , Mauro Paternostro<sup>1</sup>  and Steve Campbell<sup>4,5</sup> <sup>1</sup> Centre for Theoretical Atomic, Molecular and Optical Physics, School of Mathematics and Physics, Queen's University Belfast, Belfast BT7 1NN, United Kingdom<sup>2</sup> Departamento de Química Física, UPV/EHU, Apdo 644, E-48080 Bilbao, Spain<sup>3</sup> Department of Physics, University College Cork, Ireland<sup>4</sup> School of Physics, University College Dublin, Belfield Dublin 4, Ireland<sup>5</sup> School of Physics, Trinity College Dublin, Dublin 2, IrelandE-mail: [steve.campbell@ucd.ie](mailto:steve.campbell@ucd.ie)**Keywords:** shortcuts to adiabaticity, optimal control, quantum thermodynamics**Abstract**

We quantitatively assess the energetic cost of several well-known control protocols that achieve a finite time adiabatic dynamics, namely counterdiabatic and local counterdiabatic driving, optimal control, and inverse engineering. By employing a cost measure based on the norm of the total driving Hamiltonian, we show that a hierarchy of costs emerges that is dependent on the protocol duration. As case studies we explore the Landau–Zener model, the quantum harmonic oscillator, and the Jaynes–Cummings model and establish that qualitatively similar results hold in all cases. For the analytically tractable Landau–Zener case, we further relate the effectiveness of a control protocol with the spectral features of the new driving Hamiltonians and show that in the case of counterdiabatic driving, it is possible to further minimize the cost by optimizing the ramp.

**1. Introduction**

The inherent fragility of quantum systems necessitates that we develop methods to coherently control their evolution [1, 2]. The need for high precision control is evidently ubiquitous; the study of how and why peculiar quantum properties manifest requires techniques that allows for the careful manipulation of these systems. While a variety of techniques have been developed for many types of quantum system [1–4], often neglected has been the associated resources needed to achieve this high degree of control. While such an omission is evidently justified when one is solely interested in studying a particular quantum phenomenon, it is vital to account for such expenditures when developing novel technologies that exploit these quantum features. Indeed, recently the application of control techniques that can achieve an effective adiabatic dynamics in a finite time, called ‘shortcuts-to-adiabaticity’ [1, 2], has been shown to be highly effective in a diverse range of settings including quantum gates [5], quantum games [6, 7] nano-scale thermodynamic cycles [8–12], open quantum systems [13–16], manipulating critical many-body systems [17, 18], and quantum precision measurements [19]. This further highlights the importance of understanding the additional resources required to achieve precise control in a quantitative manner.

The question of how to quantify the necessary resources to control a quantum system using a particular protocol has recently become a topic of intense research activity (indeed, in the context of thermodynamic cycles the issue becomes more subtle since any additional energy which is not dissipated can in principle be recycled and act as a catalyst [20]). The variety of ways in which a particular set-up can be coherently controlled has led to a plethora of definitions [5, 8–11, 21–38]. Nevertheless, since many of these quantifiers invariably share some common traits, it leads to a natural question: which control protocols are the most resource intensive?

In this work we begin to tackle this issue by employing the cost measure introduced in [28] and, through it, quantitatively and qualitatively compare and contrast several different coherent control protocols. For a fixed protocol duration,  $\tau$ , naturally, one must choose a figure of merit with which to judge the success of the process.

Here we choose the target state fidelity,  $\mathcal{F} = |\langle \psi(\tau) | \Psi \rangle|^2 \rightarrow 1$ , where  $|\psi(\tau)\rangle$  is the evolved state of our system using a particular control protocol and  $|\Psi\rangle$  is the target state we are aiming to achieve. By fixing the quantifier of cost and examining the paradigmatic settings of the Landau–Zener model, which serves to elucidate the control needs of critical many-body systems [17], the parametric quantum harmonic oscillator, and the Jaynes–Cummings model, we show that a consistent hierarchy of costs can emerge. We find that techniques that suppress all non-adiabatic excitations are generally energetically costly protocols and we relate this to the effect that these more resource intensive techniques have on the energy spectrum of the controlled system. However, we show that the cost can be minimized by exploiting the freedom in choosing how one ramps the system. Furthermore, we establish that optimal control (OC) and inverse engineering (IE) protocols are generally less energetically costly.

The manuscript is organized as follows. In section 2, we outline the basic tools utilized throughout this work. Section 3 quantitatively analyzes the energetic cost of control for three paradigmatic settings: ramping the ground state of the Landau–Zener model through its avoided crossing, compressing the thermal state of a quantum harmonic oscillator, and tuning the light–matter interaction strength in the Jaynes–Cummings model. Finally, in section 4 we draw our conclusions and provide some further discussions.

## 2. Preliminaries

Controlling quantum systems such that an effective adiabatic dynamics is realized in a finite time can be achieved through a variety of techniques [1, 2, 39]. In this work, we will focus on several of the most prevalent of such protocols for a given situation and, for brevity, we refer to the comprehensive reviews on the topics for a detailed discussion of their derivations and implementations [1, 2]. Counter-diabatic (CD) or transitionless quantum driving is one such method that involves adding an additional correction term to the bare Hamiltonian,  $H_0$ , such that the resulting dynamics exactly tracks the corresponding adiabatic dynamics [40–42]. If one is only interested in controlling populations, then with a suitable choice of phase [30] this can be achieved through the CD term

$$H_{\text{CD}} = i \sum_n |\partial_t \psi_n(t)\rangle \langle \psi_n(t)|, \quad (1)$$

where  $|\psi_n(t)\rangle$  are the eigenstates of the bare system Hamiltonian one is interested in manipulating and where we assume units such that  $\hbar = 1$ . An oft-cited drawback of this approach is that the resulting correction term can be highly non-local [17, 29, 43] and therefore difficult to implement. However, for certain systems by exploiting a unitary transformation, the total  $H_0 + H_{\text{CD}}$  Hamiltonian can be re-expressed in the so-called local counter-diabatic (LCD) form,  $H_{\text{LCD}}$ , where perfect final target state fidelity is still achieved [44]. Crucially, though,  $H_{\text{LCD}}$  does not involve any complex non-local operators and is instead constructed using the same operators that appear in  $H_0$ . Another drawback of the CD approach is that, in principle, it requires full spectral knowledge. Thus often for complex systems where complete spectral information is not available, alternative approaches must be employed. In this work, when possible, we will also consider other more heuristic protocols, OC theory [45–47] and IE [1], and compare the resource intensiveness of their implementation.

Our aim is to both qualitatively and quantitatively assess the cost of implementing these protocols, which is a topic that has ignited significant interest recently [5, 8–11, 21–38]. Indeed as discussed in [2] the notion of the cost has been somewhat loosely employed and therefore different quantifiers probe different aspects of the system’s energy or its interactions. In this regard, we are in principle free to choose or define any meaningful quantifier we wish. However, we must ensure that whichever approach we use provides a sound basis for drawing a comparison. For example, simply determining the average energy of the state  $\langle \psi(t) | H_0 | \psi(t) \rangle$  is insufficient as the CD approach will appear to be free as the instantaneous energy will be identical to the adiabatic energy. Here we mainly focus on the cost as defined by Zheng *et al* [28] and use the norm of the Hamiltonian to define the instantaneous cost of the evolution

$$\partial_t \mathcal{C} = \|H_k\| \quad (2)$$

using the Frobenius norm, where  $H_k$  is the total Hamiltonian used in determining the evolution and  $k$  is used to distinguish the various protocols. Notice that [28] was concerned with determining the additional resources necessary to implement CD only and therefore defined the cost in terms of the additional energy added to the bare Hamiltonian. Here the cost is related to the norm of the full Hamiltonian implemented during the evolution and thus accounts for the *total* energy of the process, rather than only defining the energetic cost to achieve the control protocol.

A few important remarks are in order. Firstly, as we shall focus on unitary dynamics, any additional energy resources employed are not dissipated. This is a subtle issue that is particularly relevant if one wishes to extend our analysis to the performance of thermodynamic cycles [8–12], as it is possible for the additional energy

requirements invested in achieving coherent control to be recycled, see e.g. [20, 21]. Secondly, to ensure a fair comparison, we explicitly account for the bare Hamiltonian contribution to the energy requirements, thus ensuring that no evolution is free. By employing equation (2) our analysis essentially focuses on the intensity of all the driving fields in achieving high fidelity control, and while we expect the qualitative behavior to persist for other definitions of cost, this question requires nevertheless a systematic study in itself.

### 3. Case studies

#### 3.1. Landau–Zener model

To begin, we consider a single spin in a time-dependent field

$$H_0 = \Delta \frac{\sigma_x}{2} + g(t) \frac{\sigma_z}{2}. \quad (3)$$

In what follows we will assume that the system is initialized in its ground state with  $g(0) = -0.2$  and we wish to evolve through the avoided crossing to  $g(\tau) = 0.2$ . Our goal is to estimate the energy used to achieve this evolution under the condition that the fidelity at the start and end of the process is close to unity. Depending on the control protocol employed we may allow for the transient to leave the ground state manifold.

For OC the fastest approach is given by a bang-off-bang (BOB) pulse [48–50], where the system is suddenly and strongly quenched, followed by a free evolution with no field, and finally a reverse sudden quench is applied

$$g_{\text{BOB}}(t) = \begin{cases} g_Q, & t = 0, \\ 0, & 0 < t < \tau, \\ -g_Q, & t = \tau, \end{cases} \quad (4)$$

with  $g_Q \gg g(0)$  (in our simulations  $g_Q = 100$  is sufficient). This approach is effective when the evolution time is given by the quantum speed limit (QSL) time,  $\tau_{\text{QSL}}$  [39, 48, 49, 51]. However we will also consider more general approaches valid for  $\tau > \tau_{\text{QSL}}$  later. By focusing on initial and target ground states of the Landau–Zener model, equation (3), the QSL time can be found fully analytically and is given by [49]

$$\cos\left(\frac{\Delta}{2}\tau_{\text{QSL}}\right) = |\alpha_i \alpha_t| + |\beta_i \beta_t|, \quad (5)$$

where  $\alpha_{i(t)}$  and  $\beta_{i(t)}$  correspond to the  $\sigma_z$  basis coefficients of the normalized initial (target) state, respectively.

The CD control field which must be added to the bare Hamiltonian is given by [42]

$$H_{\text{CD}} = -\frac{g'(t)\Delta}{2[\Delta^2 + g^2(t)]}\sigma_y. \quad (6)$$

This control technique ensures that not only will the system be in the required state at the end of the protocol but it will also remain in the instantaneous eigenstate of the original Hamiltonian throughout. There is complete freedom in both the form of the ramp and its duration.

Turning to LCD, perfect target state fidelity can be achieved by making a unitary transformation of  $H_0 + H_{\text{CD}}$  to arrive at [14, 52]

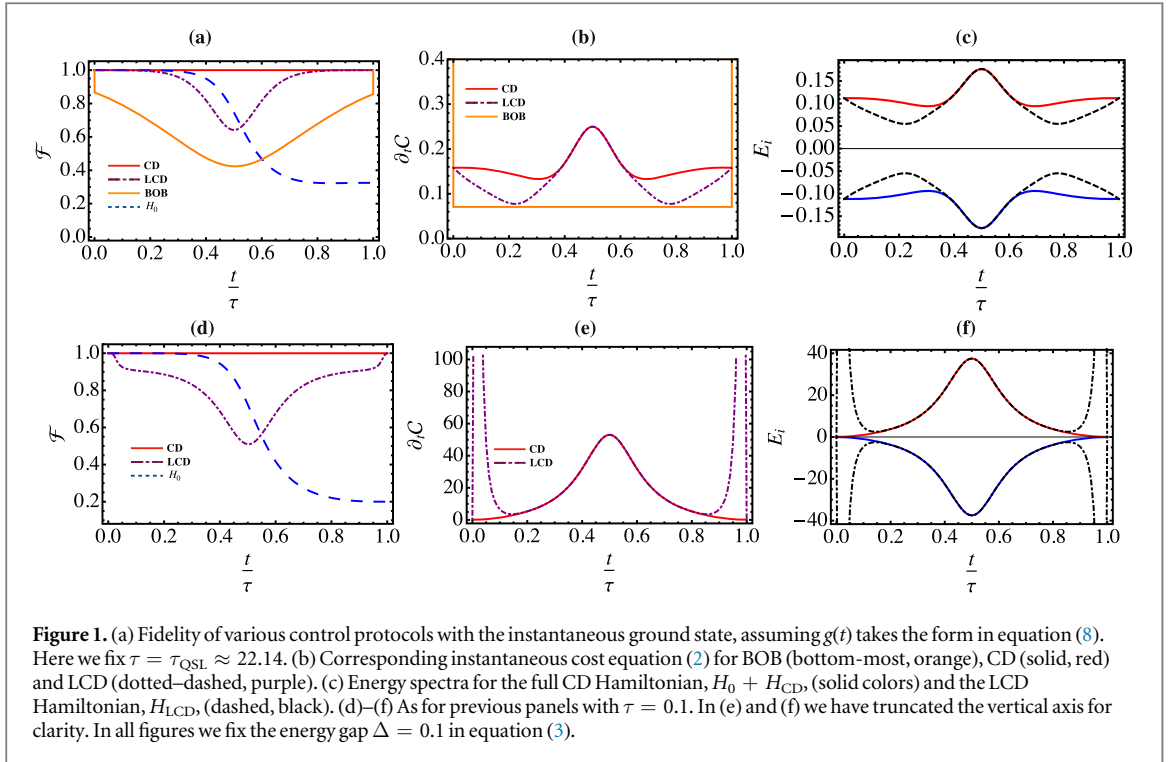
$$H_{\text{LCD}} = P(t) \frac{\sigma_x}{2} + [g(t) - \eta(t)] \frac{\sigma_z}{2}, \quad (7)$$

with  $P(t) = \sqrt{\Delta^2 + \dot{\theta}^2}$ ,  $\theta = \text{arccot}[g(t)/\Delta]$ , and  $\eta(t) = \text{arctan}(\dot{\theta}/\Delta)$ . Notice that, as with OC, the shortcut is now achieved using a Hamiltonian that is of the same general form as the bare Hamiltonian,  $H_0$ . Unlike CD, where the form of the ramp can be completely arbitrary, for the LCD term to be effective a particular form of ramp is required, one with smooth start and end points, given by [14]

$$g(t) = g_0 + 10g_d \left(\frac{t}{\tau}\right)^3 - 15g_d \left(\frac{t}{\tau}\right)^4 + 6g_d \left(\frac{t}{\tau}\right)^5, \quad (8)$$

with  $g_0 = -0.2$  and  $g_d = 0.4$ . Despite this, we can choose  $\tau$  to be arbitrarily small and, in particular, smaller than the QSL time. This shows a key difference between OC, where an optimized path for varying  $g(t)$  is found, and the LCD approach. On the one hand, we see that OC is bounded by the QSL when only the field is varied. On the other hand, with LCD we are also time-dependently varying the energy splitting,  $\Delta$ , via  $P(t)$  in equation (7) and therefore we can drive the system faster than the QSL. It is important to notice that we ‘beat’ the speed limit using CD and LCD because we are significantly altering the spectrum of the system. In essence, the more energy available to be imparted to the system the faster the evolution can be performed [29].

As mentioned, we will initialize our system in the ground state for  $g(0) = -0.2$ , the target state will be the ground state at  $g(\tau) = 0.2$  and we initially fix the gap  $\Delta = 0.1$ . We will consider the BOB pulse performed at the QSL,  $\tau = \tau_{\text{QSL}} \approx 22.14$ , while for CD and LCD, as there are no constraints on how fast the protocol can be

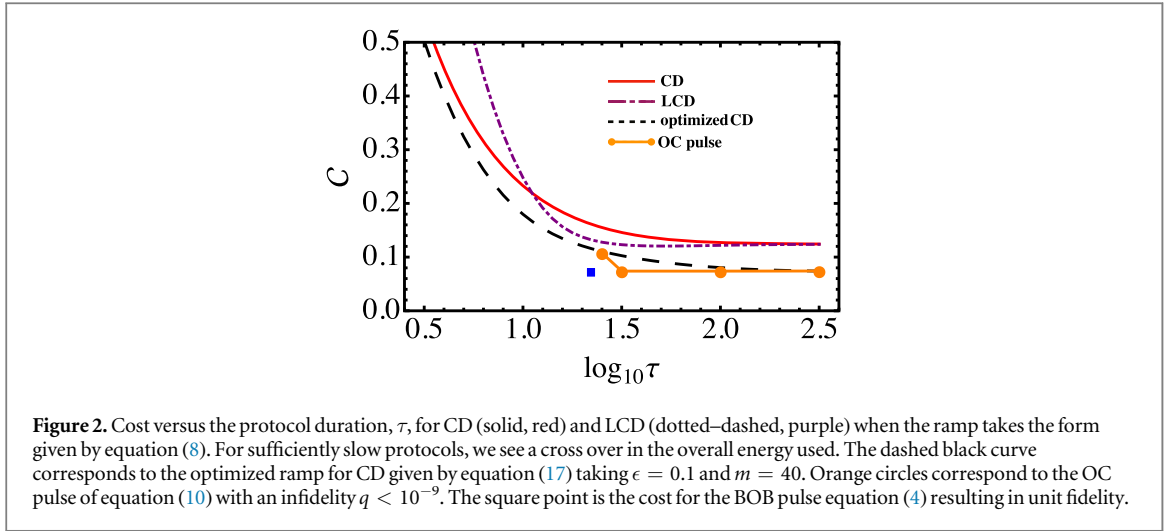


achieved we will consider,  $\tau = \tau_{\text{QSL}}$  so as to compare faithfully with BOB, and  $\tau = 0.1$ , i.e. extremely fast driving. For both CD and LCD we will employ the smooth ramp as given by equation (8).

In figure 1(a) we examine the instantaneous fidelity,  $\mathcal{F} = |\langle \psi(t) | \phi \rangle|^2$ , between the states  $|\psi(t)\rangle$  evolved according to BOB, CD, LCD, and the bare Hamiltonian, with the corresponding instantaneous adiabatic state  $|\phi\rangle$  of  $H_0$  using the ramp equation (8) with  $\tau = \tau_{\text{QSL}}$ . Clearly we see a qualitative similarity in the behavior of BOB and LCD, both protocols achieve the target state by evolving through partially excited states of the system. Figure 1(b) shows the corresponding instantaneous cost, equation (2). Immediately, and somewhat expectantly as they involve strong additional control fields, CD and LCD are resource intensive approaches. Interestingly, the BOB protocol is by far the most efficient. With the exception of two strong pulses when driving at the QSL, the system consumes comparatively little energy. It is worth noting the dichotomy between the behavior of the cost for CD and LCD compared with BOB: the former ones are maximized at the avoided crossing while the latter is minimized. For CD, as discussed in [29], the speed up facilitated by the driving term is related to a sharp increase in the speed of the dynamics near the avoided crossing. In essence, CD seeks to ‘run’ through the difficult points in the evolution, and this leads to an increase in the energy used. This can also be seen by examining the energy spectra of the control Hamiltonians themselves which are shown in figure 1(c) where the solid curves correspond to the ground and excited state for  $H = H_0 + H_{\text{CD}}$ . We see that the addition of the control field leads to the evolving Hamiltonian having an increasingly large gap. Thus, as the system is evolved according to this new Hamiltonian, it can be driven progressively faster until it reaches the avoided crossing of the original Hamiltonian. The dashed curves show the corresponding energy eigenvalues for the LCD Hamiltonian, where a similar behavior is observed throughout except at the start and end of the ramp. In contrast, BOB essentially does not have to deal with the difficulties that arise when approaching the avoided crossing as it mostly evolves according to a system with no applied field. It is interesting that when the system is evolving near the avoided crossing the instantaneous cost for both CD and LCD exhibit an identical behavior despite their respective evolved states differing greatly at these times, see figure 1(a). We find notable differences in the behavior of the instantaneous costs appear only in the earlier and later stages of the protocols and again these features are reflected in the respective energy eigenvalues of the applied Hamiltonians. These differences are very sensitive to the total protocol duration, as shown in figures 1(d)–(f) where we show the same quantities for  $\tau = 0.1$  (notice that this duration is significantly shorter than the QSL time and therefore OC only varying the field is not possible). For fast driving the LCD has very high instantaneous costs, while for longer protocols we find  $\partial_t \mathcal{C}$  can be lower for LCD compared to CD.

This last observation has an interesting consequence: if we compute the total cost, by integrating equation (2)

$$\mathcal{C} = \frac{1}{\tau} \int_0^\tau \|H_k\| dt, \quad (9)$$



we find that for fast protocols using the ramp given by equation (8) CD is less costly, as shown in figure 2. However there is a crossover. For sufficiently slow processes, but still faster than the adiabatic limit, LCD becomes the less resource intensive control method. The crossover is dependent on the value of  $\Delta$ ; we find that larger values lead to a crossover at smaller  $\tau$ .

In figure 2, we also add results obtained with an OC method that is applicable for  $\tau > \tau_{\text{QSL}}$  in which the time dependence of the control field is the sum of a linear ramp and a truncated Fourier series as

$$g_{\text{OC}}(t) = g_0 - 2g_0 \frac{t}{\tau} + \sum_{n=1}^{n_{\text{max}}} a_n \sin\left(\frac{n\pi t}{\tau} + \phi_n\right), \quad (10)$$

where  $n_{\text{max}}$  is the maximum number of Fourier components. To obtain the optimized parameters  $\{a_n, \phi_n\}$  and thus the function  $g_{\text{OC}}(t)$ , we numerically minimize the combined function:  $q^\gamma \mathcal{C}$  where  $q = 1 - \mathcal{F}$  is the final infidelity. We tune the power  $\gamma$  to best minimize simultaneously the infidelity and the cost  $\mathcal{C}$ . In our calculations we choose  $10^{-3} < \gamma < 10^{-2}$  and  $20 < n_{\text{max}} < 50$  depending on  $\tau$ . For  $\tau > \tau_{\text{QSL}} \sim 22.14$ , we are consistently able to achieve a very small infidelity of  $q < 10^{-9}$ . We find that OC is always the minimally resource intensive control technique, and more remarkably, for the considered Landau–Zener model here, the total cost appears almost independent of the protocol duration.

In the limit of  $\tau \rightarrow \tau_{\text{QSL}}$ , we find this particular OC method becomes less efficient as the number of frequencies to be retained increases very rapidly, thus indicating that the form of control pulse is becoming progressively harder to realize using a smooth function. Indeed, we know that at  $\tau_{\text{QSL}}$  the required ramp is given by the BOB pulse. Of course, this could in principle be emulated by equation (10) for sufficiently large  $n_{\text{max}}$ . We show the total cost for the BOB pulse in figure 2 (blue square) and the agreement with the OC results obtained at larger  $\tau$  is clearly evident, thus indicating the claimed invariance of the cost of OC to protocol duration. Finally, we remark that OC could also be directly applied to when both  $\Delta$  and  $g$  vary time-dependently. In such a case it is likely that  $\tau < \tau_{\text{QSL}}$  is achievable, however, evidently, this is a more involved scenario.

While we have restricted to using the smooth ramp equation (8), as noted previously, CD allows for any ramp to be used. Thus, unlike in typical OC methods where fidelity is maximized for a given protocol duration, since CD already guarantees perfect fidelity, we are able to optimize the choice of ramp which minimizes the cost. We refer to [37] where a similar approach is successfully implemented. The cost, equation (9) can be expressed in terms of  $s = t/\tau$  as

$$\mathcal{C} = \frac{1}{\tau} \int_0^\tau \|H(t)\| dt = \int_0^1 \|H_0(s) + \tau^{-1} H_{\text{CD}}(s)\| ds = \int_0^1 \left[ \sum_n E_n^2(s) + \tau^{-2} \sum_{\substack{n,d \\ n \neq a}} |A_{n,a}(s)|^2 \right]^{1/2} ds, \quad (11)$$

where  $A_{m,n} = \frac{i(m|\partial_t H_0|n\rangle)}{E_n - E_m}$  and we have used the Frobenius norm as before. Clearly the cost scales with the total time  $\tau$  and the contributions from the different Hamiltonian terms  $H_0$  and  $H_{\text{CD}}$  is evident. Note that the contribution from  $H_{\text{CD}}$  is similar to the usual criteria for adiabaticity i.e.  $\sum_{n \neq m} |A_{m,n}|^2 \ll 1$  as one would expect.

In the non-adiabatic regime (i.e. small total time  $\tau$ )

$$\mathcal{C} \approx \tau^{-1} \int_0^1 \|H_{\text{CD}}(s)\| ds. \quad (12)$$

If we define  $\|H_{\text{CD}}(s)\|$  as a Lagrangian and minimizing the corresponding action, we find the ramp with the lowest cost in this regime to be given by



$$g_{NA}(s) = \Delta \tan [c_1 \Delta(s + c_2)], \quad (13)$$

where  $c_{1,2}$  are constants of integration which are fixed by the boundary conditions of  $g(t)$ . The cost in this case is  $\mathcal{C} \approx \frac{|g_1 \Delta|}{\sqrt{2}\tau}$ . The dependence on the energy gap shows that for large  $\Delta$ , the ramp tends toward a linear pulse while for small  $\Delta$  it tends towards a delta pulses at each endpoint. Similarly, in the adiabatic regime (i.e. large  $\tau$ ) we have

$$\mathcal{C} \approx \int_0^1 \|H_0(s)\| ds, \quad (14)$$

$$= \int_0^1 \sqrt{(\Delta^2 + g(s)^2)/2} ds. \quad (15)$$

Thus the optimal ramp is a delta pulse at the endpoints, in order to fulfill the boundary conditions, and zero otherwise, so the positive integrand is as small as possible. This can be approximated by a continuous function as

$$g_A(s) = -g_0[\tanh(ms - m) + \tanh(ms)] \quad (16)$$

for  $m \gg 1$ . It simply remains to tackle intermediate values of  $\tau$ . The results for the two regimes can be combined as

$$g_C(s, \tau) = f(\tau)g_A(s) + [1 - f(\tau)]g_{NA}(s) \quad (17)$$

for monotonically increasing  $f(\tau)$  bounded between 0 and 1. One choice is  $f(\tau) = \frac{2}{\pi} \arctan(\epsilon\tau)$ , where  $\epsilon$  determines how fast one changes from one regime to another. This approach has the advantage that the total time  $\tau$  does not have to be accounted for when determining the optimal pulse. It may also prove useful in cases where calculating the norm of the full Hamiltonian is difficult but estimating the norm of the adiabatic and counterdiabatic components is more tractable.

In figure 2, the dashed black curve corresponds to CD when the ramp is given by equation (17). Thus, for the paradigmatic Landau–Zener model we see that OC is the lowest cost control technique, however, CD and LCD offer some noticeable advantages. Using these techniques, the final state fidelity is guaranteed independent of the protocol duration and these methods are applicable when arbitrarily fast control is required. For CD the associated cost can be further minimized with respect to the form of ramp employed. While this is still more costly than OC, it allows for driving times faster than the QSL which are not achievable using OC techniques that depend solely on manipulating the applied field.

### 3.2. Parametrically driven quantum harmonic oscillator

Let us now consider the case of a time-dependent harmonic oscillator, initially in thermal equilibrium at inverse temperature  $\beta = 1/(k_B T)$ , with mass  $m$  whose Hamiltonian is of the usual form

$$H_0 = \frac{p^2}{2m} + \frac{m}{2}\omega^2(t)x^2, \quad (18)$$

where  $x$  and  $p$  are the position and momentum operators, respectively, and we assume that the time-dependent frequency  $\omega(t)$  starts with initial value  $\omega_0$  at  $t = 0$  and ends with final value  $\omega_1$  at  $t = \tau$ . The state of the oscillator remains Gaussian for any driving protocol  $\omega(t)$  due to the quadratic form of the Hamiltonian. The Schrödinger equation for the parametric quantum harmonic oscillator can be solved exactly for any frequency modulation [53–55]. The system dynamics are completely determined by a dimensionless adiabaticity parameter,  $Q^*$ , as introduced by Husimi [53]

$$Q^* = \frac{1}{2\omega_0\omega(t)} \{ \omega_0^2 [\omega^2(t) X_\tau^2 + \dot{X}_\tau^2] + [\omega^2(t) Y_\tau^2 + \dot{Y}_\tau^2] \}, \quad (19)$$

where  $X_t$  and  $Y_t$  are the solutions of the force-free classical oscillator equation,  $\ddot{X}_t + \omega^2(t)X_t = 0$ , satisfying the boundary conditions  $X_0 = 0$ ,  $\dot{X}_0 = 1$  and  $Y_0 = 1$ ,  $\dot{Y}_0 = 0$ . The adiabaticity quantity  $Q^* \geq 1$  is the ratio of the nonadiabatic mean energy and the adiabatic energy and is equal to one for slow driving that realizes adiabatic transformations.

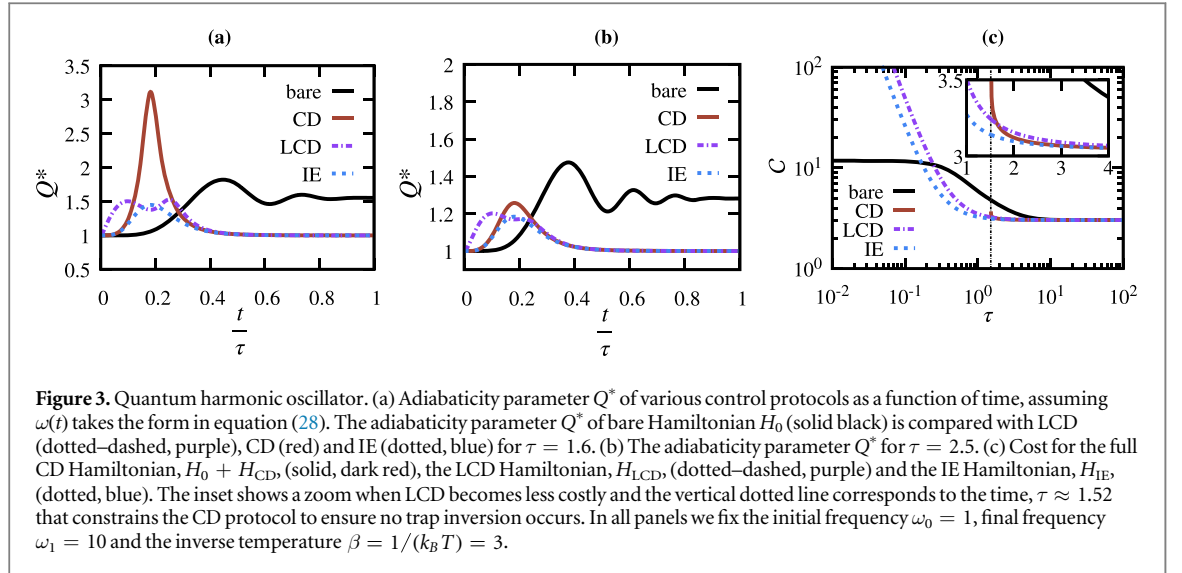
Using equation (1) we can determine the CD term [43]

$$H_{CD} = -\frac{\dot{\omega}(t)}{4\omega(t)}(xp + px), \quad (20)$$

and consequently the adiabaticity parameter can be expressed as [56]

$$Q_{CD}^* = \left[ 1 - \frac{\dot{\omega}^2(t)}{4\omega^4(t)} \right]^{-1/2}. \quad (21)$$

We note that the time variation of the frequency must fulfill the condition,  $\omega^2(t) > \dot{\omega}^2(t)/[4\omega^2(t)]$ , to avoid the trap inversion. This is consistent with the conditions in typical experimental realizations and also ensures that the adiabaticity criterion equation (19) retains a clear physical interpretation during the process.



Considering the LCD approach [1, 44, 57], similarly to the qubit case, the nonlocal CD term is mapped onto a unitarily equivalent Hamiltonian with a local potential of the form

$$H_{LCD} = \frac{p^2}{2m} + \frac{m\Omega^2(t)x^2}{2}, \quad (22)$$

with the modified time-dependent squared frequency

$$\Omega^2(t) = \omega^2(t) - \frac{3\dot{\omega}^2(t)}{4\omega^2(t)} + \frac{\ddot{\omega}(t)}{2\omega(t)}. \quad (23)$$

The exact dynamics of the system are obtained from the solution of the adiabaticity parameter, equation (19) solved by replacing  $\omega(t)$  with  $\Omega(t)$ . Again, to avoid the inversion of the harmonic trapping potential, the effective frequency  $\Omega(t)$  must be positive ( $\Omega^2(t) > 0$ ).

A final control technique that is particularly effective for the oscillator case is IE based on constructing appropriate parameter trajectories of the frequency by employing the Lewis-Riesenfeld invariants of motion [58]. Considering  $H_0$ , the dynamics are obtained by solving the Schrödinger equation based on the invariants of motion of the following form [32, 59]

$$I(t) = \frac{1}{2} \left( \frac{x^2}{b^2} m\omega_0^2 + \frac{1}{m} \pi^2 \right), \quad (24)$$

where  $\pi = bp - mbx$  plays the role of a momentum conjugate to  $x/b$ ,  $\omega_0$  and is, in principle, an arbitrary constant taken as  $\omega_0 = \omega(0)$ , and the dimensionless scaling function  $b(t)$  satisfies the Ermakov equation

$$\ddot{b}(t) + \omega^2(t)b(t) = \omega_0^2/b^3(t). \quad (25)$$

The resulting time-dependent instantaneous energy of the Hamiltonian reads

$$\langle H_{IE}(t) \rangle = \frac{1}{2} \left[ \frac{\dot{b}^2(t)}{2\omega_0} + \frac{\omega^2(t)b^2(t)}{2\omega_0} + \frac{\omega_0}{2b^2(t)} \right] \coth\left(\frac{\beta\omega_0}{2}\right), \quad (26)$$

and corresponding adiabaticity parameter is given by [10]

$$Q_{IE}^*(t) = 1 + \frac{\dot{\omega}^2(t)}{8\omega^4(t)}. \quad (27)$$

The behavior of the various adiabaticity parameters for the three considered control protocols is shown in figure 3 using a ramp analogous to equation (8) [1]

$$\omega(t) = \omega_0 + 10\omega_d \left(\frac{t}{\tau}\right)^3 - 15\omega_d \left(\frac{t}{\tau}\right)^4 + 6\omega_d \left(\frac{t}{\tau}\right)^5, \quad (28)$$

where the difference between final and initial frequency is  $\omega_d = \omega_1 - \omega_0$ . We clearly see a similarity between the methods as they all start and end at the same value of adiabaticity. However, the CD has the largest fluctuation while the behavior of the LCD and IE show significantly smaller peaks. The IE technique gives the smallest value of adiabaticity parameter which results in the smallest nonadiabatic excitation during the process. In figure 3(a) we show the adiabaticity parameter for a shorter time duration ( $\tau = 1.6$ ) and observe a large increase in the



nonadiabatic excitations than the case of  $\tau = 2.5$ , see figure 3(b). The validity CD protocol, as dictated by the constraint ensuring no trap inversion occurs, breaks down at time  $\tau \approx 1.52$ .

Turning our attention to the instantaneous cost as defined in equation (2), as the spectrum is unbounded, the resulting norm is not finite. To circumvent this issue we note that the the average energy of the system evaluated over the the full Hamiltonian will behave in a qualitatively identical manner and as such we use it as an indicator of the control cost. Thus for the oscillator, we must modify our definition of the total cost to

$$\mathcal{C} = \frac{1}{\tau} \int_0^\tau \langle H_{\text{tot}} \rangle dt, \quad (29)$$

where the full Hamiltonian for a given control protocol is [10]

$$\langle H_{\text{tot}} \rangle = \frac{\omega(t)}{\omega_0} Q_k^* \langle H(0) \rangle = \frac{\omega_t}{2} Q_k^* \coth(\beta\omega_0/2) \quad (30)$$

with  $k = \text{CD, LCD, IE}$ . We note, for the LCD, the  $\omega(t)$  is replaced with  $\Omega(t)$  in the equation above as well as in evaluation of  $Q^*$  with equation (19). In figure 3(c) we numerically evaluate the cost of the evolution for the various control protocols using ramp equation (28). We observe that while all the protocols lead to the same value of cost for long durations, they significantly differ for fast processes. We find that IE is the most efficient of the three protocols. Furthermore, in line with the Landau–Zener model, for intermediate timescales the CD performs better than the LCD but there is a crossover as the driving time becomes smaller. Thus, our results indicate that a qualitatively similar hierarchy emerges in the case of driving a thermal harmonic oscillator.

### 3.3. Jaynes–Cummings model

As a final case study, we examine the Jaynes–Cummings model [60]. Recently, owing to its richness, this model has attracted renewed interest in diverse areas such as quantum control [61, 62]. We thus consider the model [63, 64]

$$H_{\text{JC}} = \frac{\omega_A}{2} \sigma_z + \omega a^\dagger a + g(t)(a\sigma^+ + a^\dagger\sigma^-), \quad (31)$$

which describes the interaction of a two-level atom, modeled as a spin- $\frac{1}{2}$  particle, with a single mode of the electromagnetic field whose annihilation and the creation operators are  $a$  and  $a^\dagger$ , respectively. While the free Hamiltonian  $H_0 = \omega_A \sigma_z/2 + \omega a^\dagger a$  is assumed to be time-independent, the interaction Hamiltonian  $H_{\text{int}} = g(t)(a\sigma^+ + a^\dagger\sigma^-)$  depends on a time-dependent coupling rate  $g(t)$ , upon which we exert control [63–65]. As the total number of excitations in the system  $N_e \equiv |e\rangle\langle e| + a^\dagger a$  is a constant of motion, for any given initial number of photons  $n$  in the field the dynamics is restricted to the subspace spanned by states  $\{|e, n\rangle, |g, n+1\rangle\}$ . Owing to this feature equation (31) may be written as the direct sum of Hamiltonian terms  $(H_{\text{JC}})_n$  labeled by the corresponding number of photons in the field. Over the basis  $\{|e, n\rangle, |g, n+1\rangle\}$ , such terms take the form [61, 66]

$$(H_{\text{JC}})_n = \frac{1}{2} \begin{pmatrix} (2n+1)\omega + \delta & 2g(t)\sqrt{n+1} \\ 2g(t)\sqrt{n+1} & (2n+1)\omega - \delta \end{pmatrix}, \quad (32)$$

where  $\Omega_R(t) \equiv 2g(t)\sqrt{n+1}$  is the  $n$ -photon time-varying Rabi frequency and  $\delta = \omega_A - \omega$  corresponds to the detuning parameter of the radiation from the atomic resonance.

Equation (32), can be mapped to a Landau–Zener model by introducing the spin-like operators  $\bar{\sigma}^- = |g, n+1\rangle\langle e, n|$ ,  $\bar{\sigma}^+ = |e, n\rangle\langle g, n+1|$ ,  $\bar{\sigma}_z = |e, n\rangle\langle e, n| - |g, n+1\rangle\langle g, n+1|$ , so that

$$(H_{\text{JC}})_n = \frac{(2n+1)\omega}{2} \mathbb{I} + \frac{\delta}{2} \bar{\sigma}_z + \frac{\Omega_R(t)}{2} \bar{\sigma}_x. \quad (33)$$

Moreover, through a  $\pi/2$  rotation about the  $y$ -axis, we have  $\bar{\sigma}_z \rightarrow \bar{\sigma}_x$  and  $\bar{\sigma}_x \rightarrow -\bar{\sigma}_z$ , which takes us to

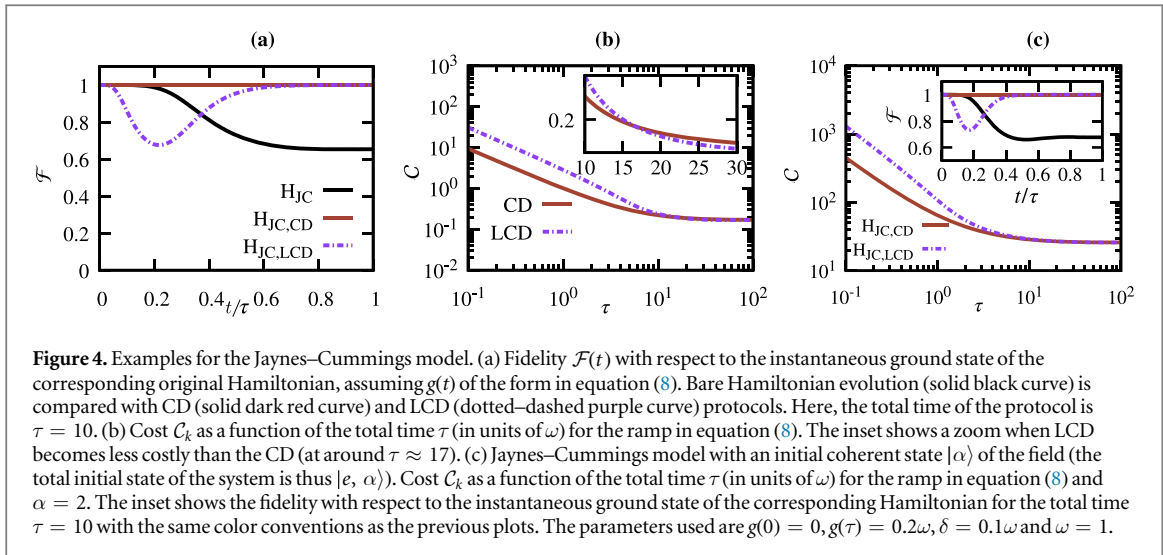
$$(H_{\text{JC}})_n = \frac{(2n+1)\omega}{2} \mathbb{I} + \frac{\delta}{2} \bar{\sigma}_x - \frac{\Omega_R(t)}{2} \bar{\sigma}_z. \quad (34)$$

From equation (34), we can already see that equations (6) and (7) are valid upon the identification of  $\Delta \rightarrow \delta$  and  $g(t) \rightarrow -\Omega_R(t)$ .

The desired CD Hamiltonian corresponding to this problem is given by [40, 42]

$$H_{\text{CD}} = i \sum_{n, \sigma=\pm} (\partial_t |n, \sigma(t)\rangle \langle n, \sigma(t)| - \langle n, \sigma(t)| \partial_t |n, \sigma(t)\rangle) |n, \sigma(t)\rangle \langle n, \sigma(t)| = \dot{\theta}_n(t) \bar{\sigma}_y, \quad (35)$$

with the mixing angle  $\theta_n(t) = \frac{1}{2} \arctan\left(\frac{\Omega_R(t)}{\delta}\right)$  and  $|n, \sigma(t)\rangle$  denoting the dressed-atom eigenstates of the original Hamiltonian. The explicit expressions of the new modified total Hamiltonian for CD and LCD are presented in the [appendix](#).



Considering again the smooth ramp of  $g(t)$  in the form of equation (8) and for the initial state  $|e, 0\rangle$ , a unitary evolution is performed from  $g(0) = 0$  to a target state at  $g(\tau) = 0.2\omega$  with initially fixed  $\delta = 0.1\omega$  and setting  $\omega = 1$ . In figure 4(a) we show the fidelity of the state evolving according to CD, LCD, and the bare Hamiltonian using ramp equation (8), with respect to the instantaneous ground state of  $(H_{JC})_{n=0}$  for  $\tau = 10$ . Again, we find a qualitative similarity in the behavior of CD and LCD when compared with the Landau–Zener model.

In figure 4(b) we show the cost by applying equations (2) and (9) for both a CD and LCD strategy and  $n = 0$  excitations (we neglect constant energy factors of  $H_{JC,CD}$  and  $H_{JC,LCD}$ ), finding it again qualitatively in line with what was observed for the Landau–Zener model (see figure 2).

In figure 4(c) we examine the cost and fidelity of the state evolving according to CD and LCD strategies starting from a coherent state  $|\alpha\rangle$  of the cavity field with the ramp in equation (8) and the amplitude  $\alpha = 2$ . Clearly we see a similarity in the behavior of both shortcut protocols with the case of vacuum initial state in perfectly achieving the target state (see inset of figure 4(c)). However, the cost of shortcut to adiabaticity protocols are higher than the vacuum state situation as more  $n$ -subspaces must be considered, in light of the form of the initial state of the field. For our calculations we have computed the cost and the fidelity using  $n = 0, \dots, 40$ . Such a cutoff is well justified as the populations of the states  $|g, m\rangle$  and  $|e, m\rangle$  with  $m > 40$  are  $p_m > 40 < 10^{-20}$ . In keeping with the previous results we once again find that, for shorter protocol durations, CD is energetically more efficient than LCD, while for larger values of  $\tau$ , the LCD strategy becomes less costly.

## 4. Conclusions

We have quantitatively compared and contrasted the energetic cost of achieving finite time adiabatic dynamics in a variety of physically relevant settings, namely the Landau–Zener model, the parametric quantum harmonic oscillator, and the Jaynes–Cummings model. By exploiting a cost function based on the norm of the driving Hamiltonian [28], we have shown that a hierarchy in the resource intensiveness emerges. For the Landau–Zener model, we have shown that OC protocols appear to be the most efficient techniques and presented a remarkable invariance to the protocol duration. Conversely, CD driving was shown to be more costly, however it allows for arbitrarily fast manipulation. We showed the manipulation of a system beyond the QSL is possible only when the system energy spectrum is affected, precisely as is the case for local and full counterdiabatic drivings. We found that the general features exhibited in the Landau–Zener case are also present in other physically relevant settings. While we have focused on one particular definition of cost, we nevertheless expect our results to qualitatively hold for other suitable choices, such as those based on excess energy [9] or work fluctuations [25]. Our analysis sheds light on the relative effectiveness of promising strategies for the control of quantum dynamics. By highlighting the respective advantages of such strategies, and the associated cost, the information provided by our study will be useful in conjunction with complementary studies on the achievable minimal control time of quantum dynamics [67] for the development of future energy-efficient quantum devices.

## Acknowledgments

The authors thank Pablo Poggi and Barış Çakmak for useful discussions. We acknowledge support from the Royal Commission for the Exhibition of 1851, the Basque Country Government (Grant No. IT986-16), the EU Collaborative project TEQ (grant agreement 766900), the DfE-SFI Investigator Programme (grant 15/IA/2864), COST Action CA15220, the Royal Society Newton Fellowship (Grant Number NF160966), the Royal Society Wolfson Research Fellowship ((RSWF\R3\183013), the Leverhulme Trust Research Project Grant (grant nr. RGP-2018-266), and the SFI Starting Investigator Research Grant (project ‘SpeedDemon’, grant nr. 18/SIRG/5508).

## Appendix

As discussed in section 3.3, the Jaynes–Cummings model can be expressed as a direct sum of  $2 \times 2$ -matrix Hamiltonians  $(H_{JC})_n$  with  $n$  excitations by resorting to the constant of motion  $\hat{N}_e$ . This allows for a direct identification with a Landau–Zener problem. For each block, one can construct a CD Hamiltonian, which reads as

$$(H_{JC,CD})_n = (H_{JC})_n + H_{CD} = \frac{(2n+1)\omega}{2}\mathbb{I} + \frac{\delta}{2}\bar{\sigma}_x - g(t)\sqrt{n+1}\bar{\sigma}_z + \frac{\dot{g}(t)\sqrt{n+1}\delta}{\delta^2 + 4(n+1)g^2(t)}\bar{\sigma}_y, \quad (36)$$

while the LCD is analogous to equation (7), which becomes (neglecting a constant energy shift)

$$(H_{JC,LCD})_n = \frac{1}{2}\sqrt{\delta^2 + \frac{4(n+1)\dot{g}^2(t)\delta^2}{(\delta^2 + 4(n+1)g^2(t))^2}}\bar{\sigma}_x \quad (37)$$

$$- \sqrt{n+1}\left(g(t) + \frac{(\delta^2 + 4(n+1)g^2(t))\dot{g}(t) - 8(n+1)g(t)\dot{g}^2(t)}{(\delta^2 + 4(n+1)g^2(t))^2 + 4(n+1)\dot{g}^2(t)}\right). \quad (38)$$

Note that the operators  $\bar{\sigma}_{x,y,z}$  refer here to the dressed atom-field basis, namely,  $\bar{\sigma}_x = |e, n\rangle\langle e, n| - |g, n+1\rangle\langle g, n+1|$ ,  $\bar{\sigma}_y = -i|e, n\rangle\langle g, n+1| + i|g, n+1\rangle\langle e, n|$  and  $\bar{\sigma}_z = -|e, n\rangle\langle g, n+1| - |g, n+1\rangle\langle e, n|$  (see section 3.3).

## ORCID iDs

Gabriele De Chiara  <https://orcid.org/0000-0003-3265-9021>

Mauro Paternostro  <https://orcid.org/0000-0001-8870-9134>

Steve Campbell  <https://orcid.org/0000-0002-3427-9113>

## References

- [1] Torrontegui E, Ibáñez S, Martínez-Garaot S, Modugno M, del Campo A, Guéry-Odelin D, Ruschhaupt A, Chen X and Muga J G 2013 Shortcuts to adiabaticity *Adv. At. Mol. Opt. Phys.* **62** 117
- [2] Guéry-Odelin D, Ruschhaupt A, Kiely A, Torrontegui E, Martínez-Garaot S and Muga J G 2019 *Shortcuts to Adiabaticity: Concepts, Methods, and Applications* arXiv:1904.08448
- [3] Bason M G, Viteau M, Malossi N, Huillery P, Arimondo E, Ciampini D, Fazio R, Giovannetti V, Mannella R and Morsch O 2012 High-fidelity quantum driving *Nat. Phys.* **8** 147
- [4] Zhang J et al 2013 Experimental implementation of assisted quantum adiabatic passage in a single spin *Phys. Rev. Lett.* **110** 240501
- [5] Santos A C and Sarandy M S 2015 Superadiabatic controlled evolutions and universal quantum computation *Sci. Rep.* **5** 15775
- [6] Sørensen J J W H et al 2016 Exploring the quantum speed limit with computer games *Nature* **532** 210–3
- [7] Sels D 2018 Stochastic gradient ascent outperforms gamers in the quantum moves game *Phys. Rev. A* **97** 040302
- [8] del Campo A, Goold J and Paternostro M 2014 More bang for your buck: super-adiabatic quantum engines *Sci. Rep.* **4** 6208
- [9] Abah O and Lutz E 2017 Energy efficient quantum machines *Europhys. Lett.* **118** 40005
- [10] Abah O and Lutz E 2018 Performance of shortcut-to-adiabaticity quantum engines *Phys. Rev. E* **98** 032121
- [11] Çakmak B and Müstecaplıoğlu Ö E 2019 Spin quantum heat engines with shortcuts to adiabaticity *Phys. Rev. E* **99** 032108
- [12] Li J, Fogarty T, Campbell S, Chen X and Busch T 2018 An efficient nonlinear feshbach engine *New J. Phys.* **20** 015005
- [13] Vacanti G, Fazio R, Montangero S, Palma G M, Paternostro M and Vedral V 2014 Transitionless quantum driving in open quantum systems *New J. Phys.* **16** 053017
- [14] Sun Z, Zhou L, Xiao G, Poletti D and Gong J 2016 Finite-time Landau–Zener processes and counterdiabatic driving in open systems: beyond Born, Markov, and rotating-wave approximations *Phys. Rev. A* **93** 012121
- [15] Dann R, Tobalina A and Kosloff R 2019 Shortcut to equilibration of an open quantum system *Phys. Rev. Lett.* **122** 250402
- [16] Alipour S, Chenu A, Rezakhani A T and del Campo A 2019 *Shortcuts to Adiabaticity in Driven Open Quantum Systems: Balanced Gain and Loss and Non-Markovian Evolution* arXiv:1907.07460
- [17] del Campo A, Rams M M and Zurek W H 2012 Assisted finite-rate adiabatic passage across a quantum critical point: exact solution for the quantum ising model *Phys. Rev. Lett.* **109** 115703
- [18] Campbell S, De Chiara G, Paternostro M, Palma G M and Fazio R 2015 Shortcut to adiabaticity in the Lipkin–Meshkov–Glick model *Phys. Rev. Lett.* **114** 177206

- [19] Pang S and Jordan A 2017 Optimal adaptive control for quantum metrology with time-dependent hamiltonians *Nat. Commun.* **8** 14695
- [20] Kosloff R and Rezek Y 2017 The quantum Harmonic otto cycle *Entropy* **19** 136
- [21] Torrontegui E, Lizuain I, González-Resines S, Tobalina A, Ruschhaupt A, Kosloff R and Muga J G 2017 Energy consumption for shortcuts to adiabaticity *Phys. Rev. A* **96** 022133
- [22] Tobalina A, Alonso J and Muga J G 2018 Energy consumption for ion transport in a segmented paul trap *New J. Phys.* **20** 065002
- [23] Horowitz J M and Jacobs K 2015 Energy cost of controlling mesoscopic quantum systems *Phys. Rev. Lett.* **115** 130501
- [24] Calzetta E 2018 Not-quite-free shortcuts to adiabaticity *Phys. Rev. A* **98** 032107
- [25] Funo K, Zhang J-N, Chatou C, Kim K, Ueda M and del Campo A 2017 Universal work fluctuations during shortcuts to adiabaticity by counterdiabatic driving *Phys. Rev. Lett.* **118** 100602
- [26] Cui Y-Y, Chen X and Muga J G 2016 Transient particle energies in shortcuts to adiabatic expansions of harmonic traps *J. Phys. Chem. A* **120** 2962–9
- [27] Demirplak M and Rice S A 2008 On the consistency, extremal, and global properties of counterdiabatic fields *J. Chem. Phys.* **129** 154111
- [28] Zheng Y, Campbell S, De Chiara G and Poletti D 2016 Cost of counterdiabatic driving and work output *Phys. Rev. A* **94** 042132
- [29] Campbell S and Deffner S 2017 Trade-off between speed and cost in shortcuts to adiabaticity *Phys. Rev. Lett.* **118** 100601
- [30] Santos A C and Sarandy M S 2017 Generalized shortcuts to adiabaticity and enhanced robustness against decoherence *J. Phys. A: Math. Theor.* **51** 025301
- [31] Herrera M, Sarandy M S, Duzzioni E I and Serra R M 2014 Nonadiabatic quantum state engineering driven by fast quench dynamics *Phys. Rev. A* **89** 022323
- [32] Chen X and Muga J G 2010 Transient energy excitation in shortcuts to adiabaticity for the time-dependent harmonic oscillator *Phys. Rev. A* **82** 053403
- [33] Impens F and Guéry-Odelin D 2019 Fast quantum control in dissipative systems using dissipationless solutions *Sci. Rep.* **9** 4048
- [34] Abah O and Paternostro M 2019 Shortcut-to-adiabaticity otto engine: A twist to finite-time thermodynamics *Phys. Rev. E* **99** 022110
- [35] Bravetti A and Tapias D 2017 Thermodynamic cost for classical counterdiabatic driving *Phys. Rev. E* **96** 052107
- [36] del Campo A, Chenu A, Deng S and Wu H 2018 *Friction-Free Quantum Machines* (Berlin: Springer) pp 127–48
- [37] Mortensen H L, Sørensen Jens J W H, Mølmer K and Sherson J F 2018 Fast state transfer in a  $\lambda$ -system: a shortcut-to-adiabaticity approach to robust and resource optimized control *New J. Phys.* **20** 025009
- [38] Bukov M, Sels D and Polkovnikov A 2019 Geometric speed limit of accessible many-body state preparation *Phys. Rev. X* **9** 011034
- [39] Deffner S and Campbell S 2017 Quantum speed limits: from heisenberg uncertainty principle to optimal quantum control *J. Phys. A: Math. Theor.* **50** 453001
- [40] Demirplak M and Rice S A 2003 Adiabatic population transfer with control fields *J. Chem. Phys.* **119** 9937
- [41] Demirplak M and Rice S A 2005 Assisted adiabatic passage revisited *J. Phys. Chem. B* **109** 6838
- [42] Berry M 2009 Transitionless quantum driving *J. Phys. A: Math. Theor.* **42** 365303
- [43] Muga J G, Chen X, Ibanez S, Lizuain I and Ruschhaupt A 2010 Transitionless quantum drivings for the harmonic oscillator *J. Phys. B: At. Mol. Opt. Phys.* **43** 085509
- [44] del Campo A 2013 Shortcuts to adiabaticity by counterdiabatic driving *Phys. Rev. Lett.* **111** 100502
- [45] Doria P, Calarco T and Montangero S 2011 Optimal control technique for many-body quantum dynamics *Phys. Rev. Lett.* **106** 190501
- [46] Caneva T, Calarco T and Montangero S 2011 Chopped random-basis quantum optimization *Phys. Rev. A* **84** 022326
- [47] Mukherjee V, Montangero S and Fazio R 2016 Local shortcut to adiabaticity for quantum many-body systems *Phys. Rev. A* **93** 062108
- [48] Caneva T, Murphy M, Calarco T, Fazio R, Montangero S, Giovannetti V and Santoro G E 2009 Optimal control at the quantum speed limit *Phys. Rev. Lett.* **103** 240501
- [49] Hegerfeldt G C 2013 Driving at the quantum speed limit: optimal control of a two-level system *Phys. Rev. Lett.* **111** 260501
- [50] Poggi P M, Lombardo F C and Wisniacki D A 2013 Quantum speed limit and optimal evolution time in a two-level system *Europhys. Lett.* **104** 40005
- [51] Frey M R 2016 Quantum speed limits—primer, perspectives, and potential future directions *Quantum Inf. Process.* **15** 3919
- [52] Stefanatos D and Paspalakis E 2019 Efficient generation of the triplet Bell state between coupled spins using transitionless quantum driving and optimal control *Phys. Rev. A* **99** 022327
- [53] Husimi K 1953 Miscellanea in elementary quantum mechanics, ii *Prog. Theor. Phys.* **9** 381–402
- [54] Deffner S and Lutz E 2008 Nonequilibrium work distribution of a quantum harmonic oscillator *Phys. Rev. E* **77** 021128
- [55] Deffner S, Abah O and Lutz E 2010 Quantum work statistics of linear and nonlinear parametric oscillators *Chem. Phys.* **375** 200–8  
Stochastic Processes in Physics and Chemistry (in honor of Peter Hänggi)
- [56] Mishima H and Izumida Y 2017 Transition probability generating function of a transitionless quantum parametric oscillator *Phys. Rev. E* **96** 012133
- [57] Deffner S, Jarzynski C and del Campo A 2014 Classical and quantum shortcuts to adiabaticity for scale-invariant driving *Phys. Rev. X* **4** 021013
- [58] Lewis H R and Riesenfeld W B 1969 An exact quantum theory of the time-dependent harmonic oscillator and of a charged particle in a time-dependent electromagnetic field *J. Math. Phys.* **10** 1458–73
- [59] Chen X, Ruschhaupt A, Schmidt S, del Campo A, Guéry-Odelin D and Muga J G 2010 Fast optimal frictionless atom cooling in harmonic traps: shortcut to adiabaticity *Phys. Rev. Lett.* **104** 063002
- [60] Jaynes E T and Cummings F W 1963 Comparison of quantum and semiclassical radiation theories with application to the beam maser *Proc. IEEE* **51** 89–109
- [61] Gerry C C and Knight P L 2005 *Introduction to Quantum Optics* (Cambridge: Cambridge University Press)
- [62] Barnett S M et al 2017 Journeys from quantum optics to quantum technology *Prog. Quantum Electron.* **54** 19–45 Special issue in honor of the 70th birthday of Professor Sir Peter Knight FRS
- [63] Joshi A and Lawande S V 1993 Generalized jaynes-cummings models with a time-dependent atom-field coupling *Phys. Rev. A* **48** 2276–84
- [64] Lawande S V and Joshi A 1994 Stochastic fluctuations in the jaynes-cummings model *Phys. Rev. A* **50** 1692–9
- [65] Law C K, Zhu S-Y and Zubairy M S 1995 Modification of a vacuum rabi splitting via a frequency-modulated cavity mode *Phys. Rev. A* **52** 4095–8
- [66] Shore B W and Knight P L 1993 The Jaynes–Cummings model *J. Mod. Opt.* **40** 1195–238
- [67] Poggi P M 2019 Geometric quantum speed limits and short-time accessibility to unitary operations *Phys. Rev. A* **99** 042116